

## **Session 5:**

### ISM DIAGNOSTICS:

Physical Conditions,  
Excitation Mechanisms, Chemistry,  
Atomic-Molecular Transition

# Molecules as tracers of galaxy evolution

Susanne Aalto<sup>1</sup>

<sup>1</sup>Department of Earth and Space Sciences, Chalmers University of Technology  
Onsala Space Observatory, SE-439 92 Onsala, Sweden  
email: [saalto@chalmers.se](mailto:saalto@chalmers.se)

**Abstract.** Studying the molecular phase of the interstellar medium in galaxies is fundamental for the understanding of the onset and evolution of star formation and the growth of supermassive black holes. We can use molecules as observational tools exploiting them as tracers of chemical, physical and dynamical conditions. In this short review, key molecules (e.g. HCN, HCO<sup>+</sup>, HNC, HC<sub>3</sub>N, CN, H<sub>3</sub>O<sup>+</sup>) in identifying the nature of buried activity and its evolution are discussed including some standard astrochemical scenarios. Furthermore, we can use IR excited molecular emission to probe the very inner regions of luminous infrared galaxies (LIRGs) allowing us to get past the optically thick dust barrier of the compact obscured nuclei, e.g. in the dusty LIRG NGC4418. High resolution studies are often necessary to separate effects of excitation and radiative transport from those of chemistry - one example is absorption and effects of stimulated emission in the ULIRG Arp220. Finally, molecular gas in large scale galactic outflows is briefly discussed.

**Keywords.** galaxies: evolution — galaxies: ISM — galaxies: active — radio lines: ISM — ISM: molecules — ISM: abundances — astrochemistry

---

## 1. Introduction

Spectacular bursts of star formation and feeding of supermassive black holes (SMBHs) occur when collisions of gas-rich galaxies funnel massive amounts of molecular gas and dust into nuclei of luminous and ultra luminous infrared galaxies (LIRGs/ULIRGs). There are several reasons why molecular emission and absorption are very useful tools to study the nature and evolution of LIRGs and ULIRGs. Molecules are fundamentally important since they serve as fuel for the evolution of galaxies through star formation and the growth of SMBHs. The discovery of molecular gas in large scale galactic outflows also suggests that molecules play a part in the turning-off of starbursts and AGNs. Furthermore, mm and submm emission can penetrate highly obscured regions allowing us to probe the dusty nuclei of (U)LIRGs revealing the nature of the buried activity.

Here, the use of molecules as tracers of extragalactic astrochemistry is introduced in section 2. Useful molecular lines are presented in section 3 and in section 4 some global line ratios and examples of spectral scans are discussed. Effects of IR radiation on molecular excitation is presented in section 5. In section 6 the importance of studying molecular chemistry and excitation at high resolution is discussed including new interferometric results on molecular gas in large scale outflows and winds.

## 2. Extragalactic astrochemistry

The CO 1–0 line is often used to trace H<sub>2</sub> mass (e.g. Paglione *et al.* 2001; Wada & Tomisaka 2005; Narayanan *et al.* 2012) and gas dynamics. The line intensity ratio between CO and the polar molecule HCN is a popular measure of the mass fraction of dense ( $n > 10^4$  cm<sup>-3</sup>) molecular gas (e.g. Gao & Solomon 2004). Astrochemistry offers

an additional new tool to study galaxy evolution - in particular in deeply dust-obscured objects. We can study both the radiative and dynamical impact on the gas properties and its chemistry and hence develop scenarios for the evolution of molecular gas in galaxies. There are a number of standard scenarios often referred to when we discuss extragalactic astrochemistry:

(a) **Photon (or Photo) dominated region (PDR)** – Regions affected by far-ultraviolet photons (energy  $h\nu=6\text{--}13.6$  eV). The surface temperatures may be large (300–1000 K) but bulk temperatures are expected to be moderate (20–50 K) due to the layered structure of the PDR. The chemistry is dominated by photo-chemistry (e.g. Hollenbach & Tielens 1997). The penetration of the UV photons is limited by dust and, as  $A_V$  increases, cosmic rays take over as the dominant source of ionization reactions. The heating occurs through photoelectric effect on grains and PAHs, collisional de-excitation of  $\text{H}_2$ .

(b) **X-ray dominated region (XDR)** – These regions are affected by X-rays with  $h\nu=1\text{--}100$  keV providing a larger penetration depth than in PDRs and a more efficient heating mechanism. Thus XDRs are signified by large bulk temperatures  $> 100$  K and a chemical structure typical of the special ion-neutral chemistry triggered by the irradiation of X-rays (e.g. Maloney *et al.* 1996; Lepp & Dalgarno 1996; Meijerink & Spaans 2005). The ionization occurs through primary X-rays and secondary photo electrons. The heating occurs through Coulomb heating,  $\text{H}_2$  ionization,  $\text{H}_2$  vibrational excitation, and dissociative excitation. The ionization rate is high (from the secondary photo electron).

(c) **Cosmic ray dominated region (CDR or CRDR)** – Regions of elevated ( $> 10^3 \times$  Galactic value) cosmic ray energy density (e.g. Suchkov *et al.* 1993; Meijerink *et al.* 2011; Bayet *et al.* 2011) primarily originating from supernovae.

(d) **Dense shielded regions** In warm, dusty and dense regions, that are relatively shielded from harmful radiation, hot core-like chemistry may dominate with temperatures ranging from 50 to 500 K (e.g. Nomura & Millar 2004; Viti 2005). Icy grain mantles are released affecting chemistry and the intense infrared (IR) radiation fields impact the molecular excitation (Costagliola & Aalto 2010; Sakamoto *et al.* 2010). Formation and survival of complex species result in rich chemistry.

(e) **Mechanically dominated region** The chemistry reflects the speed of the shock and thus the level of grain processing (e.g. Usero *et al.* 2007; Viti *et al.* 2011; Kazandjian *et al.* 2012). Milder shocks results in the icy mantles coming off - and in more violent shocks the grain cores may be affected. Shock temperatures can be very high ranging from 100 K (C-shocks) up to a few thousand K (J-shocks). The dissipation of turbulence act on the bulk of the gas and may heat the gas to C-shock temperatures.

It is likely that within one resolving beam we have multiple scenarios represented. However, we have a large variety of spectral tools at our disposal allowing us to probe a wide range of physical environments, temperatures and densities of the interstellar medium. Combining molecular species and transitions with spatial resolution and sensitivity will enable us to disentangle chemical scenarios and to separate effects of excitation and radiative transfer from those of chemistry.

### 3. Some useful molecular emission lines and ratios

A summary of molecular species detected in extragalactic sources can be found in Martín *et al.* (2011). By 2011, a total of 46 species and 23 isotopic variants had been identified. With the advent of ALMA this list will grow significantly in the coming years. Intensity ratios of emission lines between species are often used to identify various astrochemical scenarios and/or physical conditions in the gas. Below is a list of a few popular molecular lines and ratios.

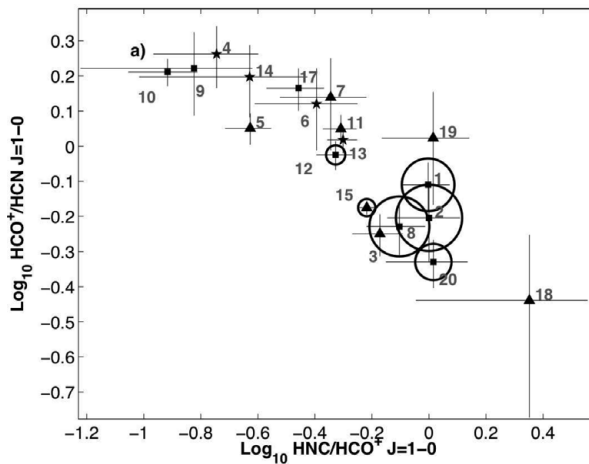


**Figure 1.** Plot of the  $\text{HCO}^+/\text{HCN}$  vs. the  $\text{HNC}/\text{HCO}^+$  1–0 line ratio for a sample of luminous LIRGs, ULIRGs and AGNs (Costagliola *et al.* 2011). The circles indicate galaxies with  $\text{HC}_3\text{N}$  10–9 detections where the diameter of the circle is proportional to the  $\text{HC}_3\text{N}$  10–9/ $\text{HCN}$  1–0 line ratio. Error bars show 1- $\sigma$  uncertainties. The  $\text{HC}_3\text{N}$  luminous galaxies are also HNC-bright with respect to  $\text{HCO}^+$  and HCN. The lines were observed simultaneously with the IRAM 30m EMIR receiver.

• **Molecular ions:  $\text{HCO}^+$  and  $\text{H}_3\text{O}^+$**   
 In the molecular cores around some AGNs elevated  $\text{HCN}/\text{HCO}^+$  1–0 intensity ratios have been found (e.g. Kohno 2003; Imanishi *et al.* 2009) and also in some ULIRGs (Graciá-Carpio *et al.* 2006). A suggested interpretation is that this is a chemical effect due to the presence of an XDR. However, theoretical models are not in agreement on whether the  $\text{HCO}^+$  abundance is suppressed or enhanced relative to HCN in XDRs (e.g. Maloney *et al.* 1996; Meijerink & Spaans 2005). Furthermore,  $\text{HCN}/\text{HCO}^+$  1–0 abundance ratios  $>1$  are also expected in dense shielded gas (e.g. Aalto *et al.* 2007a) and in gas heated by shocks (e.g. Kazandjian *et al.* 2012). Thus, it is possible that  $\text{HCN}/\text{HCO}^+$  1–0 ratios are generally enhanced in compact molecular regions towards galaxy nuclei - regardless of the nature of the buried activity. For  $\text{H}_3\text{O}^+$ , models predict an order of magnitude greater abundances in XDRs than in PDRs. The first extragalactic 364 GHz detections seem to support this notion (van der Tak *et al.* 2008; Aalto *et al.* 2011). It is however possible that elevated  $\text{H}_3\text{O}^+/\text{H}_2\text{O}$

ratios are also consistent with CDRs - this requires further investigation.

• **Isomers: HNC** In cold ( $T < 24$  K) gas  $\text{HNC}/\text{HCN}$  abundance ratios are expected to be greater than unity while in dense, warmer gas and in shocked gas  $X(\text{HCN}) > X(\text{HNC})$  (Schilke *et al.* 1992). However, in XDRs and PDRs  $X(\text{HCN}) \gtrsim X(\text{HNC})$  also in warm gas (Meijerink & Spaans 2005) which complicates the use of the  $\text{HCN}/\text{HNC}$  abundance ratio as a tracer of gas temperature. Surveys reveal that global  $\text{HCN}/\text{HNC}$  1–0 intensity ratios in luminous galaxies often range between 1 and 6 (e.g. Aalto *et al.* 2002; Baan *et al.* 2010), but there are cases where the  $\text{HNC}/\text{HCN}$  3–2 intensity ratio exceeds unity (Aalto *et al.* 2007b, 2009). The cause for this “overluminosity” of HNC (e.g. in Arp 220 - see Fig. 3) has been suggested to be either due to excitation and/or to effects of IR-pumping of HNC (see section on excitation below). In some XDR models the HNC abundances may also exceed those of HCN by a factor of two, but for this effect to lead to  $I(\text{HNC}) > I(\text{HCN})$  the optical depth of the lines has to be fairly low.

• **Shielded gas: HC<sub>3</sub>N** Surveys have revealed a subset of luminous galaxies with unusually bright HC<sub>3</sub>N 10–9 emission compared to HCN 1–0 (Lindberg *et al.* 2011; Costagliola *et al.* 2011). HC<sub>3</sub>N is destroyed by UV and particle radiation, and in the Galaxy it can be found in high abundance in hot cores and in general in dense, warm and shielded gas. Interestingly, surveys reveal bright HC<sub>3</sub>N line emission from LIRGs/ULIRGs with deep IR silicate absorption features and warm FIR colours suggesting a preference for dust obscured galaxies with high  $A_V$  and deeply buried (young?) activity.

• **Radicals: CN** In contrast to HC<sub>3</sub>N, enhancement of CN is expected in XDRs and in PDRs (e.g. Aalto *et al.* 2002; Baan *et al.* 2010; Meijerink & Spaans 2005). CN is also chemically linked to HCN via photodissociation. The abundance enhancement of CN over HCN is greater in an XDR (factors 40 - 1000) than in a PDR (CN/HCN abundance ratio range from 0.5 to 2) (Lepp & Dalgarno 1996; Meijerink & Spaans 2005). Other radicals, such as CH, NO and OH are also more enhanced (relative to HCN) in an XDR than in a PDR and the CH/HCN column density for example may exceed  $10^3$ .

• **Shock tracers: SiO, H<sub>2</sub>O, HNCO, CH<sub>3</sub>OH** Shocks can form SiO through the sputtering of Si from silicate grain cores, followed by reactions between the released Si and O<sub>2</sub> or OH (Guillet *et al.* 2009). The shock must therefore be strong enough to get the Si off the grains while species such

as H<sub>2</sub>O, HNCO, CH<sub>3</sub>OH can be released in milder events resulting in the icy grain mantle coming off and releasing them into the gas phase.

• **Gas temperature: NH<sub>3</sub>, H<sub>2</sub>CO** The relative populations of the  $K_a$  ladders of the (slightly) asymmetric top molecule H<sub>2</sub>CO are generally governed by collisions and inter-ladder line ratios are thus generally good tracers of the gas kinetic temperature. Mühle *et al.* (2007) observed para-H<sub>2</sub>CO in the starburst M82 to deduce the presence of 200 K molecular gas. The inversion-rotation transitions of NH<sub>3</sub> may also be used to accurately determine gas kinetic temperature (e.g. Martin & Ho 1986).

• **Isotopologues** Isotopic variants (isotopologues) of species (e.g. <sup>13</sup>C, <sup>18</sup>O, <sup>15</sup>N) can help measure optical depth variations and thus map out the structure of the interstellar medium and find changes in the physical conditions. For example, variations in the CO/<sup>13</sup>CO 1–0 intensity ratio that map the dynamical effects on clouds in spiral arms and bars and/or effects of temperature gradients (e.g. Meier *et al.* 2000; Tosaki *et al.* 2002; Aalto *et al.* 1997, 2010; Hirota *et al.* 2010). Globally the CO/<sup>13</sup>CO 1–0 intensity ratio increases rather strongly with dust temperature, an effect that can largely be explained as a gas temperature effect (e.g. Aalto *et al.* 1995; Costagliola *et al.* 2011). Studying isotopic variants will also give important information on stellar nucleosynthesis and the number of stellar generations the ISM has gone through.

Note that these are emission lines in the mm and submm regime - a more complete list would for example include absorption line diagnostics and higher-frequency lines observed by e.g. *Herschel* (van der Werf *et al.* 2010; González-Alfonso *et al.* 2010). For example, Meijerink *et al.* (2011) suggest observing a combination of species, OH<sup>+</sup>, OH, H<sub>2</sub>O<sup>+</sup>, H<sub>2</sub>O and H<sub>3</sub>O<sup>+</sup>, to distinguish between CDRs and XDRs - many of these species are best studied at THz frequencies with the *Herschel* telescope or with ALMA.

#### 4. Global line ratios and spectral scans

There are a large number of studies using global molecular line ratios to attempt to classify galaxies in terms of nuclear activity and evolutionary status (e.g. Aalto *et al.*

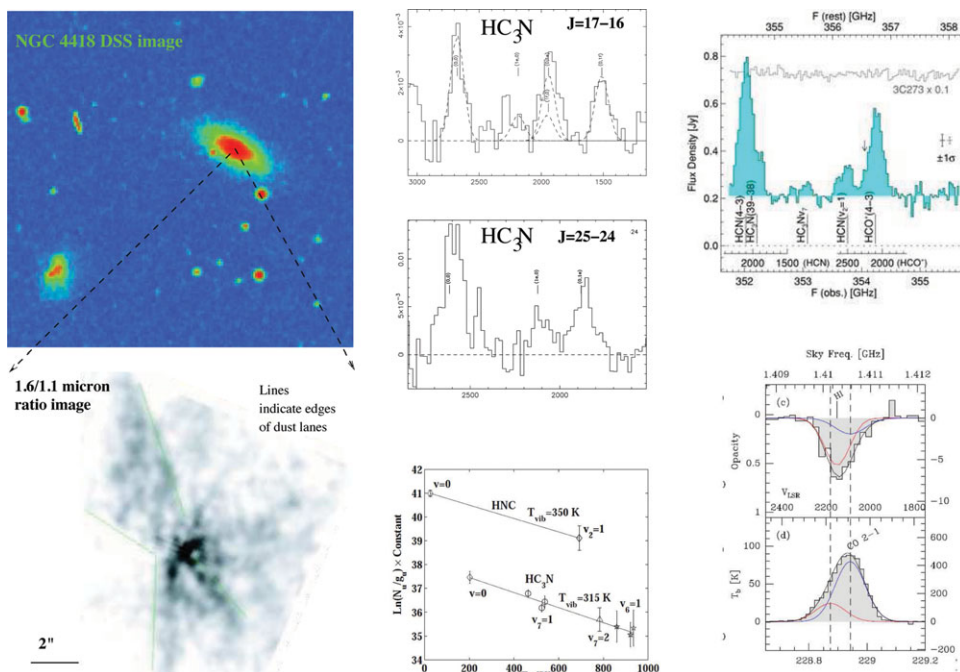


**Figure 2.** Upper left: DSS image of the LIRG NGC4418. Lower left: NICMOS NIR image of the ratio of the 1.6/1.1  $\mu\text{m}$  continuum revealing the dusty interior of NGC4418 (Evans *et al.* 2003). Upper center: Two spectra of intense HC<sub>3</sub>N emission - rotational and vibrational - from NGC4418 and below the spectra is a rotational diagram of HC<sub>3</sub>N and HNC. Upper right: SMA spectrum with HCN 4-3 and  $v_2=1$ , HCO<sup>+</sup> 4-3, HC<sub>3</sub>N 39-38 and  $v_7=1$  (Sakamoto *et al.* 2010). Lower right: MERLIN HI absorption (top) and SMA CO 2-1 emission showing evidence for infalling gas towards the nucleus of NGC4418 (Costagliola *et al.*, 2012, submitted)

1995; Paglione *et al.* 2001; Aalto *et al.* 2002; Gao & Solomon 2004; Graciá-Carpio *et al.* 2006; Krips *et al.* 2008; Baan *et al.* 2010; Papadopoulos *et al.* 2010) Although effects of radiative transfer and excitation are difficult to account for in these surveys, they are useful in identifying trends and searching for correlations. These relations may then be further explored with multi-transition observations as well as higher resolution studies.

The new broadband receivers - mounted on interferometers such as the SMA, PdBI and ALMA, and on single dish telescopes including the IRAM 30m telescope - allow several lines to be measured simultaneously improving the accuracy of the line ratios. One such example is the EVOLUTION study on the IRAM 30m where the 3mm EMIR backend was used to study the spectral properties of 25 infrared luminous galaxies selected from the IR PAH (polycyclic aromatic hydrocarbons)-silicate diagnostic diagram of Spoon *et al.* (2007). Simultaneous observations of HCN, HCO<sup>+</sup>, HNC, HC<sub>3</sub>N, C<sub>2</sub>H, SiO and CO, <sup>13</sup>CO, C<sup>18</sup>O, CN were carried out to look for correlations (Costagliola *et al.* 2011). The HCO<sup>+</sup>/HCN 1-0 ratio is correlated with the PAH equivalent width suggesting that there is a connection to PDRs. However, in general it was found that HNC and HCO<sup>+</sup> 1-0 emission appear anti correlated (see Fig. 1). This is difficult to explain with standard PDR models, and it is suggested that mechanical heating must be added to the models (e.g. Baan *et al.* 2010; Costagliola *et al.* 2011; Meijerink *et al.* 2011). All HNC-bright objects are either luminous IR galaxies (LIRG) or Seyferts. Galaxies with bright PAH emission show low HNC/HCO<sup>+</sup> ratios. Note, however, that variations in the ratios between HCN, HNC and HCO<sup>+</sup> are relatively small. Stronger effects are obtained for fainter species

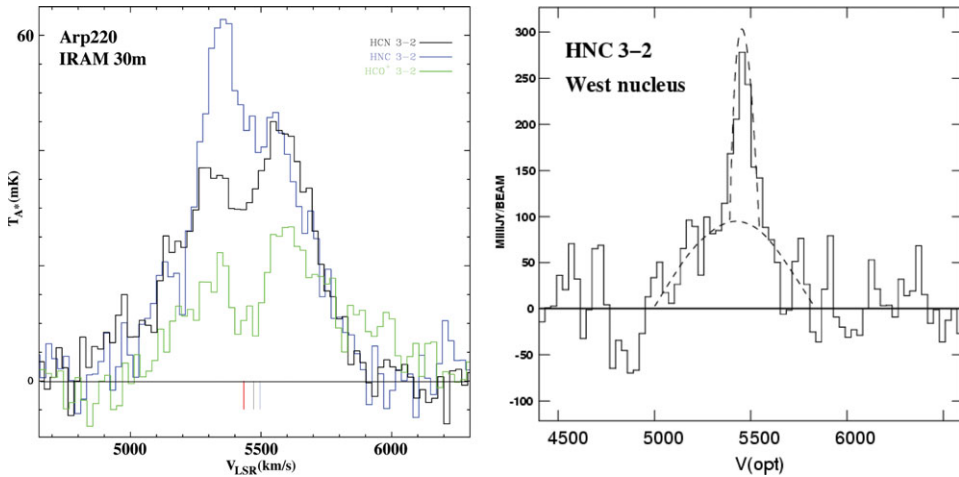


**Figure 3.** Left: Single dish (global profile) EMIR 1mm spectra of Arp220 showing  $I(\text{HNC}) > I(\text{HCN}) > I(\text{HCO}^+)$  3–2 (S. Aalto *et al.* in prep.). Right: SMA HNC 3–2 spectrum of the western nucleus of Arp220 revealing a bright narrow feature suggested to be due to weak amplification of HNC (Aalto *et al.* 2009). (The emission feature coincides with a deep absorption feature in the  $\text{HCO}^+$  3–2 spectrum (Sakamoto *et al.* 2009).) Note the difference in velocity scales: the SMA HNC spectrum is in optical velocity which is approximately  $100 \text{ km s}^{-1}$  larger than the velocities for the radio definition in the left figure.

such as  $\text{HC}_3\text{N}$ . The only  $\text{HC}_3\text{N}$  detections are in objects with  $\text{HCO}^+/\text{HCN}$  1–0 intensity ratios  $< 1$  (see Fig. 1). Galaxies with the highest  $\text{HC}_3\text{N}/\text{HCN}$  ratios have warm IRAS colours ( $60/100 \mu\text{m} > 0.8$ ) and it is suggested that  $\text{HC}_3\text{N}$  is a tracer of young, dust enshrouded activity.

#### 4.1. Spectral scans

Combining many lines simultaneously in a spectral scan will give a more complete (and complex) picture of the chemical status of a galaxy. This includes emission from rarer species with clearer diagnostic value. Spectral scans of the nearby starburst galaxies NGC253 and M82, and the starburst/Seyfert NGC1068 have been carried out at 1, 2 and 3 mm wavelength by the IRAM 30m and the Nobeyama 45m telescopes (e.g. Martín *et al.* 2006; Nakajima *et al.* 2011; Aladro *et al.* 2011, 2012). The chemistry of NGC 253 shows a similarity to that of the Galactic Center molecular clouds, which are thought to be dominated by low-velocity shocks. In contrast, the surveys of M82 reveal a PDR chemistry different from that of NGC253. For NGC1068 some of the carbon-chemistry appears similar to that of M82 while other aspects of the chemistry seem to be dominated by cosmic rays and XDRs. The ULIRG Arp220 has been surveyed in the 1mm band by the SMA interferometer (Martín *et al.* 2011) and the chemical composition seems consistent with an ISM heated by a young starburst and chemically enriched by consecutive bursts of star formation. Vibrationally excited emission from  $\text{HC}_3\text{N}$  and  $\text{CH}_3\text{CN}$  are indicative of a warm, intense IR field. With ALMA there is an ongoing spectral scan (bands 3, 6, 7, PI:Costagliola) of the LIRG NGC4418 where the spectrum is dominated by many rotational-vibrational lines of  $\text{HC}_3\text{N}$  (Aalto *et al.* 2007a; Costagliola & Aalto 2010; Sakamoto *et al.* 2010).

## 5. Molecular excitation - IR pumping of molecules

When we interpret mm and submm molecular spectra from external galaxies we usually assume that the excitation is dominated by collisions with  $\text{H}_2$ . However, there are also other possible mechanisms including IR radiative excitation where molecules absorb IR continuum corresponding to their bending modes. It is possible that this IR-pumping may affect the excitation of the rotational levels in the vibrational ground state. Thus, to correctly interpret the molecular emission we must examine its excitation. For example, both HCN and HNC can absorb IR-photons to the bending mode (its first vibrational state) and then it decays back to the ground state via its P-branch ( $\nu = 1-0$ ,  $\Delta J = +1$ ) or R-branch ( $\nu = 1-0$ ,  $\Delta J = -1$ ). In this way, a vibrational excitation may produce a change in the rotational state in the ground level and can be treated (effectively) as a collisional excitation in the statistical equations. Thus, IR pumping excites the molecule to the higher rotational level by a selection rule  $\Delta J = 2$ . For HNC, the bending mode occurs at  $\lambda = 21.5 \mu\text{m}$  ( $464.2 \text{ cm}^{-1}$ ) with an energy level  $h\nu/k = 669 \text{ K}$  and an  $A$ -coefficient of  $A_{\text{IR}} = 5.2 \text{ s}^{-1}$ . For HCN the mode occurs at  $\lambda = 14 \mu\text{m}$  ( $713.5 \text{ cm}^{-1}$ ), energy level  $h\nu/k = 1027 \text{ K}$  and  $A_{\text{IR}} = 1.7 \text{ s}^{-1}$ . The pumping of HNC and HCN may start to become effective when the IR background reaches an optically thick brightness temperature of  $T_{\text{B}} \approx 50 \text{ K}$  and  $85 \text{ K}$  respectively - and for gas densities below critical.

Furthermore, recent results toward dust obscured galaxies show the presence of rotational lines from vibrationally excited HCN,  $\text{HC}_3\text{N}$  and (tentatively) HNC (Aalto *et al.* 2007a; Costagliola & Aalto 2010; Sakamoto *et al.* 2010; Martín *et al.* 2011). *These lines can be used to probe inside the optically thick dust cocoons in the nuclei of deeply obscured galaxies. One example of this is NGC4418 where the vibrational temperatures  $T_{\text{vib}}$  of HCN, HNC and  $\text{HC}_3\text{N}$  are 200-400 K suggesting the presence of a "hot core" heated either by an extremely compact young starburst or an embedded AGN. The size of this core has been determined to be  $r < 5 \text{ pc}$ .*

## 6. Molecules at high spatial resolution

Interferometric studies provide both spatial resolution and sufficient pointing accuracy to allow us to separate regions of different dominant chemical processes. High resolution studies on IC 342 and Maffei 2 (Meier & Turner 2005, 2012) show that the HCN, HNC,  $\text{HCO}^+$  1-0 line emission and 3 mm continuum are tightly spatially correlated, indicating a close connection to star formation. In contrast, HNCO, and  $\text{CH}_3\text{OH}$  follow the molecular bar arms, especially the bar ends. This is probably caused by the spiral and bar shocks resulting in the icy grain mantles coming off. The  $\text{C}_2\text{H}$  emission prefers the starburst region (but is somewhat more extended) in Maffei 2 where it also is tracing a nuclear outflow. In IC342,  $\text{C}_2\text{H}$  is instead found near the nuclear star cluster (more evolved star formation) and not the current star formation.

There have been many studies of the chemistry of the nearby Seyfert galaxy NGC1068. High resolution interferometric observations of SiO and CN (García-Burillo *et al.* 2010) reveal that SiO is detected in a 400 pc circumnuclear disk (CND) around the AGN with SiO abundances ( $10^{-9}$ ) more than one order of magnitude above those measured in the starburst ring. The overall abundance of CN in the CND is also high,  $10^{-7}$ . Abundances measured for CN and SiO and the correlation of CN/CO and SiO/CO ratios with hard X-ray irradiation suggest that the CND of NGC1068 has become a giant XDR.

### 6.1. Molecular excitation - the compact nuclei of Arp220

To correctly interpret molecular line ratios it is important to separate effects of excitation from those of chemistry. In some cases this can only be done at high spatial resolution.

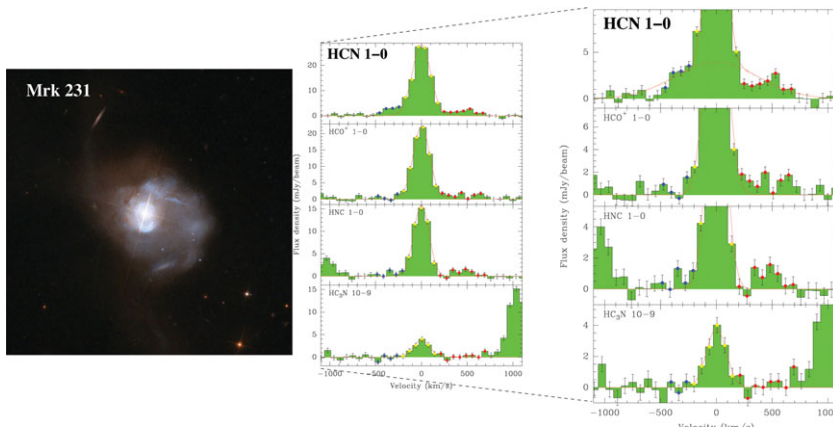


**Figure 4.** Left: HST image of Mrk231. Center and Right: Plateau de Bure interferometric spectra of HCN,  $\text{HCO}^+$ , HNC 1–0 and  $\text{HC}_3\text{N}$  10–9. In the right panels we have zoomed in on the base of the line to show the line wings more clearly. Red solid lines show Gaussian fits to the line center line widths. In the top right panel two Gaussians are fitted (Aalto *et al.* 2012a).

In the ULIRG Arp220 the  $\text{HCN}/\text{HCO}^+$  1–0 ratio is  $>1$  at  $1''.6$  resolution (Imanishi *et al.* 2007) - this is suggested to be caused either by XDR chemistry and/or by IR pumping of HCN. However, a study at even higher resolution ( $0''.4$ ) and at higher frequency ( $J=3-2$  transition) of  $\text{HCO}^+$  in Arp220 reveal an interesting effect: a big part of the  $\text{HCO}^+$  spectrum is missing towards the eastern and western nuclei due to deep absorption toward the continuum (Sakamoto *et al.* 2009). The spectra are reminiscent of P-Cygni profiles and are indicative of outflowing gas from the two ULIRG nuclei. The absorption affects the global profile of  $\text{HCO}^+$  3–2 and it must be taken into account when drawing any conclusions on what is causing elevated  $\text{HCN}/\text{HCO}^+$  intensity ratios in Arp220.

Interestingly, the HNC 3–2 profile towards the western nucleus has a prominent, narrow emission feature where  $\text{HCO}^+$  shows absorption. This may constitute the *first ever detection of an HNC maser* - even if the amplification is weak (Aalto *et al.* 2009). This maser emission may be pumped by the  $21.5 \mu\text{m}$  continuum emission. Recently a possible methanimine ( $\text{H}_2\text{CNH}$ ) maser (Rickert *et al.* 2011) has been detected towards the same source.

## 6.2. Molecular outflows

Outflows driven by AGNs and/or starbursts represent a strong and direct mechanism for feedback that may clear central regions—or the whole galaxy—of fuel for future star formation or black hole (BH) growth. Many galactic winds and outflows carry large amounts of molecular gas and dust with them. There is a growing list of examples of molecular gas in outflows including: Early type galaxies: NGC1266 (Alatalo *et al.* 2011), NGC1377 (Aalto *et al.* 2012b); Interacting starburst LIRGs: NGC3256 (Sakamoto *et al.* 2006; Sakamoto 2012), M82 (Nakai *et al.* 1987; Walter *et al.* 2002), NGC2146 (Greve *et al.* 2000; Tsai *et al.* 2009); NGC253 (e.g. García-Burillo *et al.* 2000); NGC 1614 (García-Burillo *et al.* 2012, in prep.); ULIRGs and AGNs: Mrk231 (e.g. Fischer *et al.* 2010; Feruglio *et al.* 2010; Aalto *et al.* 2012a; Cicone *et al.* 2012); M51 (Matsushita *et al.* 2007); LIRG and ULIRG surveys: (e.g. Baan 2007; Chung *et al.* 2011; Sturm *et al.* 2011); and high redshift QSOs: SWIRE survey (e.g. Polletta *et al.* 2011; Nesvadba *et al.* 2011).

Studying the physical and chemical conditions of the outflowing molecular gas will help us understand the driving mechanism, origin of the gas and its fate in the wind. Detection

of bright SiO emission in a supershell and chimney of M82 (García-Burillo *et al.* 2001) show shock processed dust grain chemistry in the starburst wind. Imaging of low- $J$  CO lines in the extreme, high-velocity wind of the QSO ULIRG Mrk231 (e.g. Feruglio *et al.* 2010; Cicone *et al.* 2012) can be used to study the excitation of the lower density gas in the outflow. Interestingly, the Mrk 231 outflow has very bright HCN 1–0 emission (Aalto *et al.* 2012a) (see Fig. 4) and emission from HNC and HCO<sup>+</sup> 1–0 is also detected in the outflow. Very recent PdBI imaging shows that the broad line wings are also present in the HCN 3–2 and 2–1 spectra (Aalto *et al.* in prep.). The HCN 1–0 flux actually rivals that of CO 1–0 in the outflow - so, why is HCN so bright? There are several options: a) Large numbers of dense clumps in the outflow. b) Extremely large HCN abundances and c) mid-IR pumping of HCN. If the outflow is extended beyond the reach of an optically thick mid-IR source of at least 85 K then c) can be ruled out. The low CO excitation (Cicone *et al.* 2012) indicates that only some of the volume can be filled with dense clumps which leaves a combination of a) and b). High HCN abundances are expected in warm regions, e.g. in AGNs (e.g. Harada *et al.* 2010) or in shocks (e.g. Tafalla *et al.* 2010; Kazandjian *et al.* 2012) and a possibility is that elevated HCN luminosity is a signature of AGN-driven outflows.

## References

- Aalto, S., Beswick, R., & Jütte, E. 2010, *A&A*, 522, A59  
 Aalto, S., Booth, R. S., Black, J. H., & Johansson, L. E. B. 1995, *A&A*, 300, 369  
 Aalto, S., Costagliola, F., van der Tak, F., & Meijerink, R. 2011, *A&A*, 527, A69  
 Aalto, S., Garcia-Burillo, S., Muller, S., *et al.* 2012a, *A&A*, 537, A44  
 Aalto, S., Monje, R., & Martín, S. 2007a, *A&A*, 475, 479  
 Aalto, S., Muller, S., Sakamoto, K., *et al.* 2012b, *A&A*, 546, A68  
 Aalto, S., Polatidis, A. G., Hüttemeister, S., & Curran, S. J. 2002, *A&A*, 381, 783  
 Aalto, S., Radford, S. J. E., Scoville, N. Z., & Sargent, A. I. 1997, *ApJ*, 475, L107  
 Aalto, S., Spaans, M., Wiedner, M. C., & Hüttemeister, S. 2007b, *A&A*, 464, 193  
 Aalto, S., Wilner, D., Spaans, M., *et al.* 2009, *A&A*, 493, 481  
 Aladro, R., Martín, S., Martín-Pintado, J., *et al.* 2011, *A&A*, 535, A84  
 Aladro, R., Viti, S., Bayet, E., *et al.* 2012, ArXiv e-prints  
 Alatalo, K., Blitz, L., Young, L. M., *et al.* 2011, *ApJ*, 735, 88  
 Baan, W. A. 2007, *New A Rev.*, 51, 149  
 Baan, W. A., Loenen, A. F., & Spaans, M. 2010, *A&A*, 516, A40  
 Bayet, E., Williams, D. A., Hartquist, T. W., & Viti, S. 2011, *MNRAS*, 414, 1583  
 Chung, A., Yun, M. S., Naraynan, G., Heyer, M., & Erickson, N. R. 2011, *ApJ*, 732, L15+  
 Cicone, C., Feruglio, C., Maiolino, R., *et al.* 2012, *A&A*, 543, A99  
 Costagliola, F. & Aalto, S. 2010, *A&A*, 515, A71  
 Costagliola, F., Aalto, S., Rodriguez, M. I., *et al.* 2011, *A&A*, 528, A30  
 Evans, A. S., Becklin, E. E., Scoville, N. Z., *et al.* 2003, *AJ*, 125, 2341  
 Feruglio, C., Maiolino, R., Piconcelli, E., *et al.* 2010, *A&A*, 518, L155+  
 Fischer, J., Sturm, E., González-Alfonso, E., *et al.* 2010, *A&A*, 518, L41  
 Gao, Y. & Solomon, P. M. 2004, *ApJS*, 152, 63  
 García-Burillo, S., Martín-Pintado, J., Fuente, A., & Neri, R. 2000, *A&A*, 355, 499  
 García-Burillo, S., Martín-Pintado, J., Fuente, A., & Neri, R. 2001, *ApJ*, 563, L27  
 García-Burillo, S., Usero, A., Fuente, A., *et al.* 2010, *A&A*, 519, A2  
 González-Alfonso, E., Fischer, J., Isaak, K., *et al.* 2010, *A&A*, 518, L43  
 Graciá-Carpio, J., García-Burillo, S., Planesas, P., & Colina, L. 2006, *ApJ*, 640, L135  
 Greve, A., Neininger, N., Tarchi, A., & Sievers, A. 2000, *A&A*, 364, 409  
 Guillet, V., Jones, A. P., & Pineau Des Forêts, G. 2009, *A&A*, 497, 145  
 Harada, N., Herbst, E., & Wakelam, V. 2010, *ApJ*, 721, 1570

- Hirota, A., Kuno, N., Sato, N., *et al.* 2010, *PASJ*, 62, 1261
- Hollenbach, D. J. & Tielens, A. G. G. M. 1997, *ARA&A*, 35, 179
- Imanishi, M., Nakanishi, K., Tamura, Y., Oi, N., & Kohno, K. 2007, *AJ*, 134, 2366
- Imanishi, M., Nakanishi, K., Tamura, Y., & Peng, C. 2009, *AJ*, 137, 3581
- Kazandjian, M. V., Meijerink, R., *et al.* 2012, *A&A*, 542, A65
- Kohno, K. 2003, in *Astronomical Society of the Pacific Conference Series*, Vol. 289, *The Proceedings of the IAU 8th Asian-Pacific Regional Meeting*, Volume 1, ed. S. Ikeuchi, J. Hearnshaw, & T. Hanawa, 349–352
- Krips, M., Neri, R., García-Burillo, S., *et al.* 2008, *ApJ*, 677, 262
- Lepp, S. & Dalgarno, A. 1996, *A&A*, 306, L21
- Lindberg, J. E., Aalto, S., Costagliola, F., *et al.* 2011, *A&A*, 527, A150
- Maloney, P. R., Hollenbach, D. J., & Tielens, A. G. G. M. 1996, *ApJ*, 466, 561
- Martin, R. N. & Ho, P. T. P. 1986, *ApJ*, 308, L7
- Martín, S., Krips, M., Martín-Pintado, J., *et al.* 2011, *A&A*, 527, A36
- Martín, S., Mauersberger, R., Martín-Pintado, J., Henkel, C., & García-Burillo, S. 2006, *ApJS*, 164, 450
- Matsushita, S., Muller, S., & Lim, J. 2007, *A&A*, 468, L49
- Meier, D. S. & Turner, J. L. 2005, *ApJ*, 618, 259
- Meier, D. S. & Turner, J. L. 2012, *ApJ*, 755, 104
- Meier, D. S., Turner, J. L., & Hurt, R. L. 2000, *ApJ*, 531, 200
- Meijerink, R. & Spaans, M. 2005, *A&A*, 436, 397
- Meijerink, R., Spaans, M., Loenen, A. F., & van der Werf, P. P. 2011, *A&A*, 525, A119
- Mühle, S., Seaquist, E. R., & Henkel, C. 2007, *ApJ*, 671, 1579
- Nakai, N., Hayashi, M., Handa, T., *et al.* 1987, *PASJ*, 39, 685
- Nakajima, T., Takano, S., Kohno, K., & Inoue, H. 2011, *ApJ*, 728, L38
- Narayanan, D., Krumholz, M. R., Ostriker, E. C., & Hernquist, L. 2012, *MNRAS*, 2537
- Nesvadba, N. P. H., Polletta, M., Lehnert, M. D., *et al.* 2011, *MNRAS*, 415, 2359
- Nomura, H. & Millar, T. J. 2004, *A&A*, 414, 409
- Paglione, T. A. D., Wall, W. F., Young, J. S., *et al.* 2001, *ApJS*, 135, 183
- Papadopoulos, P. P., van der Werf, P., Isaak, K., & Xilouris, E. M. 2010, *ApJ*, 715, 775
- Polletta, M., Nesvadba, N. P. H., Neri, R., *et al.* 2011, *A&A*, 533, A20
- Rickert, M., Momjian, E., Sarma, A., & AO Arp 220 Team. 2011, in *Bulletin of the American Astronomical Society*, Vol. 43, *American Astronomical Society Meeting Abstracts #217*, #332.01
- Sakamoto, K. 2012, ArXiv e-prints
- Sakamoto, K., Aalto, S., Evans, A. S., Wiedner, M. C., & Wilner, D. J. 2010, *ApJ*, 725, L228
- Sakamoto, K., Aalto, S., Wilner, D. J., *et al.* 2009, *ApJ*, 700, L104
- Sakamoto, K., Ho, P. T. P., & Peck, A. B. 2006, *ApJ*, 644, 862
- Schilke, P., Walmsley, C. M., Pineau Des Forets, G., *et al.* 1992, *A&A*, 256, 595
- Spoon, H. W. W., Marshall, J. A., Houck, J. R., *et al.* 2007, *ApJ*, 654, L49
- Sturm, E., González-Alfonso, E., Veilleux, S., *et al.* 2011, *ApJ*, 733, L16+
- Suchkov, A., Allen, R. J., & Heckman, T. M. 1993, *ApJ*, 413, 542
- Tafalla, M., Santiago-García, J., Hacar, A., & Bachiller, R. 2010, *A&A*, 522, A91
- Tosaki, T., Hasegawa, T., Shioya, Y., Kuno, N., & Matsushita, S. 2002, *PASJ*, 54, 209
- Tsai, A.-L., Matsushita, S., Nakanishi, K., *et al.* 2009, *PASJ*, 61, 237
- Usero, A., García-Burillo, S., Martín-Pintado, J., Fuente, A., & Neri, R. 2007, *New A Rev.*, 51, 75
- van der Tak, F. F. S., Aalto, S., & Meijerink, R. 2008, *A&A*, 477, L5
- van der Werf, P. P., Isaak, G., Meijerink, R., *et al.* 2010, *A&A*, 518, L42
- Viti, S. 2005, in *IAU Symposium*, Vol. 231, *Astrochemistry: Recent Successes and Current Challenges*, ed. D. C. Lis, G. A. Blake, & E. Herbst, 67–76
- Viti, S., Jimenez-Serra, I., Yates, J. A., *et al.* 2011, *ApJ*, 740, L3
- Wada, K. & Tomisaka, K. 2005, *ApJ*, 619, 93
- Walter, F., Weiss, A., & Scoville, N. 2002, *ApJ*, 580, L21